

SCIENTIFIC REPORTS

OPEN

Asymmetrical ligand-induced cross-regulation of chemokine (C-X-C motif) receptor 4 by α_1 -adrenergic receptors at the heteromeric receptor complex

Xianlong Gao¹, Lauren J. Albee¹, Brian F. Volkman², Vadim Gaponenko³ & Matthias Majetschak^{1,4}

Recently, we reported that chemokine (C-X-C motif) receptor (CXCR)4 and atypical chemokine receptor 3 regulate α_1 -adrenergic receptors (α_1 -AR) through the formation of hetero-oligomeric complexes. Whether α_1 -ARs also regulate chemokine receptor function within such heteromeric receptor complexes is unknown. We observed that activation of α_{1b} -AR within the α_{1b} -AR:CXCR4 heteromeric complex leads to cross-recruitment of β -arrestin2 to CXCR4, which could not be inhibited with AMD3100. Activation of CXCR4 did not cross-recruit β -arrestin2 to α_{1b} -AR. A peptide analogue of transmembrane domain 2 of CXCR4 interfered with α_{1b} -AR:CXCR4 heteromerization and inhibited α_{1b} -AR-mediated β -arrestin2 cross-recruitment. Phenylephrine (PE) induced internalization of CXCR4 in HEK293 cells co-expressing CXCR4 and α_{1b} -AR and of endogenous CXCR4 in human vascular smooth muscle cells (hVSMC). The latter was detectable despite blockade of CXCR4 with the neutralizing antibody 12G5. hVSMC migrated towards CXCL12 and PE, but not towards a combination of CXCL12 and PE. PE inhibited CXCL12-induced chemotaxis of hVSMC (IC_{50} : 77 ± 30 nM). Phentolamine cross-inhibited CXCL12-induced chemotaxis of hVSMC, whereas AMD3100 did not cross-inhibit PE-induced chemotaxis. These data provide evidence for asymmetrical cross-regulation of CXCR4 by α_1 -adrenergic receptors within the heteromeric receptor complex. Our findings provide mechanistic insights into the function of α_1 -AR:CXCR4 heteromers and suggest alternative approaches to modulate CXCR4 in disease conditions.

Chemokine (C-X-C motif) receptor (CXCR) 4 fulfills pleiotropic roles in the immune system and is regarded as an important regulator of directed cell migration¹. Based on the involvement of CXCR4 in various disease processes, such as cancer metastases, HIV infection or inflammatory diseases, multiple drugs targeting CXCR4 are currently under development and the CXCR4 antagonist AMD3100 is already approved by the Federal Drug Administration to mobilize hematopoietic stem cells in cancer patients¹⁻⁵. CXCR4 is a typical G protein-coupled receptor (GPCR)¹. Upon binding to its cognate ligand CXCL12, CXCR4 couples to guanine nucleotide-binding protein α_i ($G\alpha_i$) and also recruits β -arrestin 1/2 to the receptor, leading to termination of G protein-mediated signaling, receptor internalization and activation of G protein-independent signaling pathways^{1,6}. Several lines of evidence suggest that CXCR4 can form hetero-oligomeric complexes with other GPCRs, such as chemokine (C-C motif) receptor (CCR)2, CCR5, CXCR3, atypical chemokine receptor (ACKR) 3, chemerin receptor 23, β_2 -adrenergic receptor (AR), δ -opioid receptor or cannabinoid receptor 2, which is thought to alter the pharmacological properties of the interacting receptor partners⁷⁻¹⁴. Recently, we provided evidence that hetero-oligomeric

¹Burn and Shock Trauma Research Institute, Department of Surgery, Loyola University Chicago Stritch School of Medicine, Maywood, Illinois, 60153, USA. ²Department of Biochemistry, Medical College of Wisconsin, Milwaukee, Wisconsin, 53226, USA. ³Department of Biochemistry and Molecular Genetics, University of Illinois at Chicago, Chicago, Illinois, 60607, USA. ⁴Department of Molecular Pharmacology and Therapeutics, Loyola University Chicago Stritch School of Medicine, Maywood, Illinois, 60153, USA. Correspondence and requests for materials should be addressed to M.M. (email: mmajetschak@luc.edu)

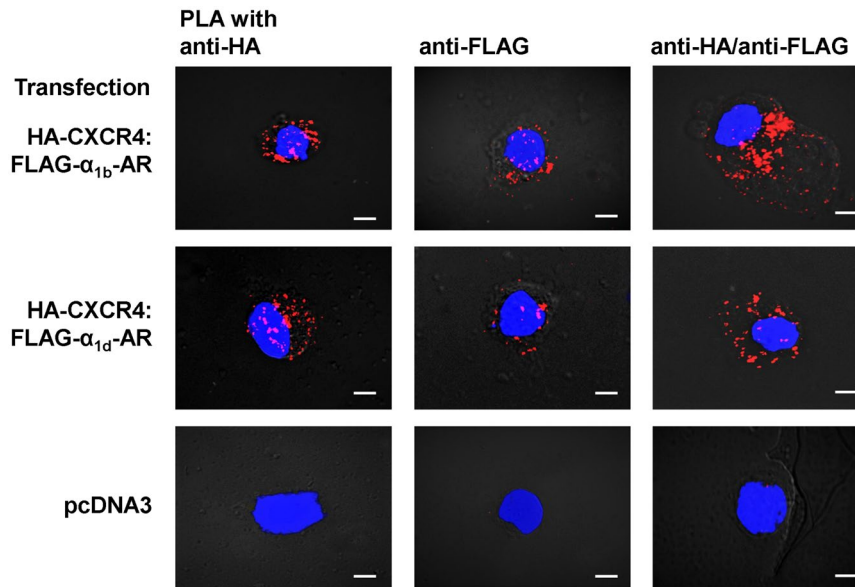


Figure 1. HA-CXCR4 forms heteromeric complexes with FLAG- $\alpha_{1b/d}$ -AR in HEK293T cells. Typical PLA images for the detection of individual receptors (left and center) and receptor-receptor interactions (right) in HEK293T cells transfected with DNA encoding HA- and/or FLAG-tagged receptors, as indicated. PLA was performed with anti-HA and anti-FLAG. pcDNA3: control, cells were transfected with empty vector. Images show merged PLA/4',6-diamidino-2-phenylindole dihydrochloride (DAPI) signals. Scale bars: 10 μ m. Images are representative of $n = 3$ independent experiments.

complexes between CXCR4, ACKR3 and α_1 -AR are constitutively expressed on the cell surface of human vascular smooth muscle cells (hVSMC), which appear to be essential for normal α_1 -AR function and through which the chemokine receptors upon agonist stimulation diametrically regulate α_1 -AR signaling and function^{15–17}. The effects of such hetero-oligomerization on CXCR4-mediated signaling and function, however, remain unknown. Here, we provide evidence for asymmetrical ligand-induced cross-regulation of CXCR4 by α_1 -AR within heteromeric CXCR4: α_1 -AR complexes in hVSMC.

Results and Discussion

α_{1b} -AR within the CXCR4: α_{1b} -AR heteromeric complex cross-recruits β -arrestin 2 to CXCR4. To reconfirm that recombinant CXCR4 and $\alpha_{1b/d}$ -AR form heteromeric complexes, we co-transfected HEK293T cells with plasmids encoding human influenza hemagglutinin (HA)-tagged CXCR4 (HA-CXCR4) and with plasmids encoding FLAG-tagged α_{1b} -AR (FLAG- α_{1b} -AR) or FLAG- α_{1d} -AR. We then performed proximity ligation assays (PLA) to visualize individual receptors and receptor-receptor interactions at single molecule resolution with anti-HA and anti-FLAG antibodies. Consistent with our previous observations^{15–17}, we observed positive signals for interactions between HA-CXCR4 and FLAG- $\alpha_{1b/d}$ -AR (Fig. 1). Next, we utilized the PRESTO-Tango cell system, which permits monitoring of β -arrestin 2 recruitment to a specific receptor¹⁸, to assess whether the CXCR4: $\alpha_{1b/d}$ -AR interaction affects β -arrestin 2 recruitment upon agonist activation of each receptor partner. We first co-expressed FLAG- $\alpha_{1b/d}$ -AR-Tango with pcDNA3 or HA-CXCR4, confirmed HA-CXCR4 expression and comparable FLAG- $\alpha_{1b/d}$ -AR-Tango expression by flow cytometry (Supplementary Fig. S1) and determined the dose-response for β -arrestin 2 recruitment upon stimulation with the selective α_1 -AR agonist phenylephrine (PE). As shown in Fig. 2a, the EC₅₀ for PE-induced β -arrestin 2 recruitment to α_{1b} -AR-Tango was 172 μ M (95% confidence interval (CI): 143–202 μ M) and the top plateau 90 ± 2 relative luminescence units (RLU)% in cells transfected with α_{1b} -AR/pcDNA3. In cells co-transfected with α_{1b} -AR-Tango/CXCR4, potency and efficacy of PE to recruit β -arrestin 2 to α_{1b} -AR were significantly reduced, as compared to cells co-transfected with α_{1b} -AR/pcDNA3 (EC₅₀: 475 (95%CI: 290–807) μ M, $p = 0.0001$; top plateau: 23 ± 3 RLU, $p < 0.0001$). Because there were no differences in PE-induced β -arrestin 2 recruitment to α_{1d} -AR in cells co-transfected with α_{1d} -AR-Tango and pcDNA3 or CXCR4 (Fig. 2b), the observed effects appear to be specific for the α_{1b} -AR:CXCR4 interaction.

While reduced β -arrestin 2 recruitment to α_{1b} -AR-Tango in the presence of CXCR4 could be explained by inhibition of α_{1b} -AR-Tango by CXCR4 through allosteric interactions within the heteromeric receptor complex, it could also be explained by cross-recruitment of β -arrestin 2 to CXCR4 upon α_{1b} -AR-Tango activation. To explore this possibility, we then co-transfected cells with α_{1b} -AR-Tango and pcDNA3 or with α_{1b} -AR-Tango and CXCR4-Tango. Despite comparable α_{1b} -AR-Tango expression under both conditions (Supplementary Fig. S2), we detected that the efficacy and potency of PE to induce β -arrestin 2 recruitment was significantly increased in cells co-transfected with α_{1b} -AR-Tango and CXCR4-Tango, as compared with cells co-transfected with α_{1b} -AR-Tango and pcDNA3 (α_{1b} -AR-Tango/pcDNA3: EC₅₀ (95%CI) 218 (130–276) μ M, top plateau: 110 ± 7 RLU%; α_{1b} -AR-Tango/CXCR4-Tango: EC₅₀ (95%CI) 22 (9–53) μ M - $p = 0.0027$, top plateau: 178 ± 11 RLU% - $p = 0.03$) (Fig. 3a).

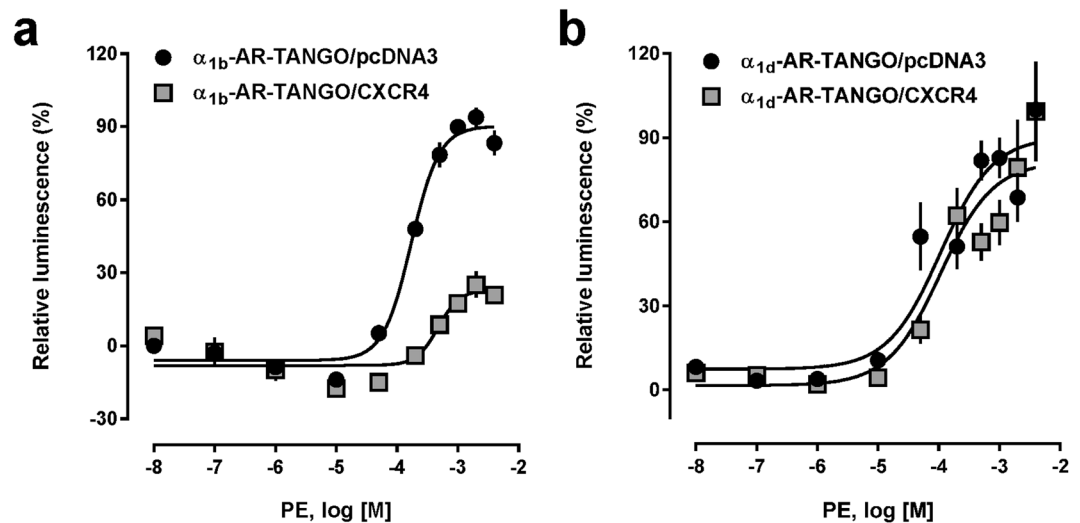


Figure 2. β -arrestin 2 recruitment to $\alpha_{1b/d}$ -AR in the presence and absence of CXCR4. HTLA cells were co-transfected with 0.75 μ g DNA encoding FLAG- α_{1b} -AR-TANGO (a) or FLAG- α_{1d} -AR-TANGO (b) plus 0.75 μ g pcDNA3 or HA-CXCR4. PE: phenylephrine. (a) β -arrestin 2 recruitment assay (PRESTO-Tango). Black circles: cells transfected with FLAG- α_{1b} -AR-TANGO/pcDNA3; grey squares: cells transfected with FLAG- α_{1b} -AR-TANGO/HA-CXCR4. N = 3 independent experiments. (b) β -arrestin 2 recruitment assay (PRESTO-Tango). Black circles: cells transfected with FLAG- α_{1d} -AR-TANGO/pcDNA3; grey squares: cells transfected with FLAG- α_{1d} -AR-TANGO/HA-CXCR4. N = 3 independent experiments.

As these data suggested that activation of α_{1b} -AR recruits β -arrestin 2 to α_{1b} -AR and CXCR4, we then expressed CXCR4-Tango in combination with α_{1b} -AR or pcDNA, confirmed comparable CXCR4-Tango expression by flow cytometry (Supplementary Fig. S2) and measured β -arrestin 2 recruitment to CXCR4 upon PE stimulation. As shown in Fig. 3b, PE did not recruit β -arrestin 2 to CXCR4-Tango when co-expressed with pcDNA3, but recruited β -arrestin 2 to CXCR4-Tango when co-expressed with α_{1b} -AR. Interestingly, the potency of PE for β -arrestin 2 recruitment to CXCR4-Tango under these conditions (EC_{50} : 20.5 (95%CI: 9–45) μ M) was ~ 10 -fold higher than the potency of PE for β -arrestin 2 recruitment to α_{1b} -AR-Tango co-transfected with pcDNA3 and ~ 20 -fold higher than the potency of PE for β -arrestin 2 recruitment to α_{1b} -AR-Tango co-transfected with CXCR4. Similarly, the efficacy of PE to recruit β -arrestin 2 to CXCR4-Tango under these conditions was 2-fold higher than the efficacy of the cognate CXCR4 agonist CXCL12 (Fig. 3b). The presence of α_{1b} -AR, however, did not affect potency and efficacy of CXCL12 to recruit β -arrestin 2 to CXCR4-Tango (Fig. 3b). Similarly, there were no differences in CXCL12-induced β -arrestin 2 recruitment to CXCR4-Tango when comparable levels of CXCR4-Tango (Supplementary Fig. S2) were co-expressed with α_{1b} -AR or α_{1b} -AR-Tango in parallel experiments (Fig. 3c). In contrast to PE, CXCL12 failed to cross-recruit β -arrestin 2 to α_{1b} -AR-Tango in cells co-expressing CXCR4 and α_{1b} -AR-Tango (Fig. 3c).

To further consolidate that agonist stimulation of α_{1b} -AR leads to cross-recruitment of β -arrestin 2 to CXCR4, we then tested the effects of the selective α_1 -AR antagonist phentolamine and of the selective CXCR4 antagonist AMD3100 on PE-induced β -arrestin 2 cross-recruitment to CXCR4-Tango. AMD3100 inhibited CXCL12 induced β -arrestin 2 recruitment to CXCR4-Tango (Fig. 4a). While AMD3100 did not inhibit PE-induced β -arrestin 2 recruitment to CXCR4-Tango in cells co-expressing CXCR4-Tango and α_{1b} -AR, phentolamine inhibited PE-induced β -arrestin 2 recruitment under these conditions (Fig. 4b). Measurements of cell viability demonstrated that phentolamine was not cytotoxic at the concentration that was used in the β -arrestin 2 recruitment assays (Fig. 4c).

Peptide analogues of transmembrane domains (TM) of GPCRs have previously been shown to interfere with receptor heteromerization and function and we reported that a peptide analogue of transmembrane domain 2 (TM2) of CXCR4 selectively interferes with CXCR4: α_{1b} -AR heteromerization in hVSMC (15–17). Thus, we tested whether the TM2 peptide analogue would also disrupt recombinant CXCR4: α_{1b} -AR heteromeric complexes and affect PE-induced β -arrestin 2 cross-recruitment to CXCR4. We used a TM4 peptide analogue of CXCR4 as a control peptide because we observed previously that this peptide analogue did not disrupt heteromerization between CXCR4: α_{1b} -AR¹⁷. As shown in Fig. 5a,b, the TM2 peptide analogue significantly reduced PLA signals corresponding to CXCR4-Tango: α_{1b} -AR interactions, as compared with vehicle-treated cells and cells treated with the TM4 peptide analogue. The TM4 peptide analogue did not significantly reduce PLA signals for CXCR4-Tango: α_{1b} -AR interactions. In parallel experiments with cells co-expressing CXCR4-Tango and α_{1b} -AR, we detected that the TM2 peptide reduced the potency of PE for β -arrestin 2 recruitment to CXCR4 3-fold, as compared with cells treated with vehicle (EC_{50} (95%CI): vehicle – 22^{17–28} μ M; TM2 – 66 (47–93) μ M, $p < 0.001$) (Fig. 5c). In contrast, the TM4 peptide analogue did not inhibit PE-induced β -arrestin 2 recruitment to CXCR4, when compared with vehicle treated cells in parallel experiments (Fig. 5d). While the TM2 peptide analogue did not interfere with PE-induced β -arrestin 2 recruitment in cells expressing α_{1b} -AR-Tango alone, it

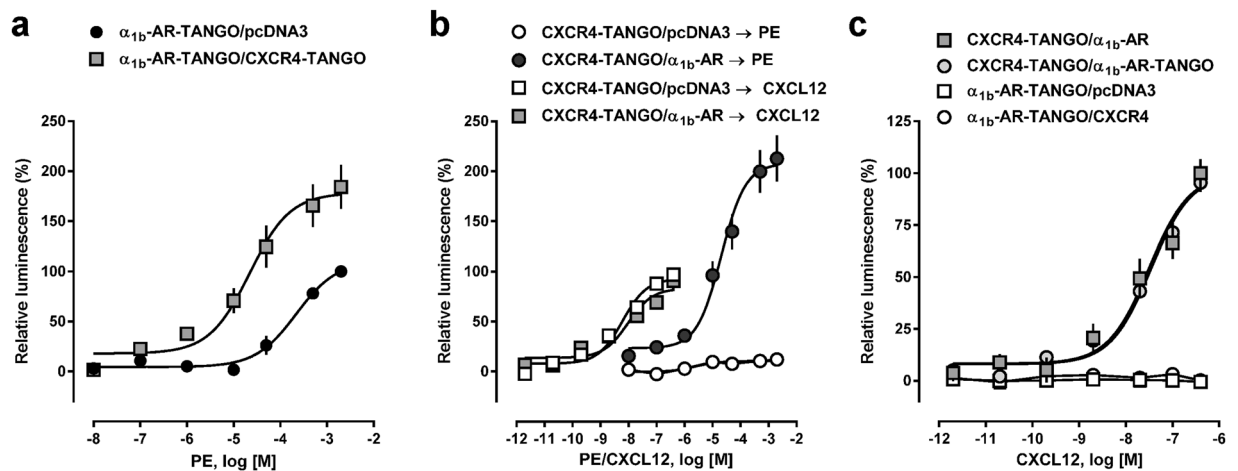


Figure 3. Activation of α_{1b} -AR leads to cross-recruitment of β -arrestin 2 to CXCR4. HTLA cells were co-transfected with FLAG- α_{1b} -AR-TANGO plus pcDNA or Myc-CXCR4-TANGO (a), FLAG-CXCR4-TANGO plus pcDNA or HA- α_{1b} -AR (b) or with FLAG-CXCR4-TANGO plus HA- α_{1b} -AR or Myc- α_{1b} -AR-TANGO or with FLAG- α_{1b} -AR-TANGO plus pcDNA3 or HA-CXCR4 (c) (0.75 μ g DNA each). PE: phenylephrine. (a) β -arrestin 2 recruitment assay (PRESTO-Tango). Black circles: cells transfected with FLAG- α_{1b} -AR-TANGO/pcDNA3; grey squares: cells transfected with FLAG- α_{1b} -AR-TANGO/CXCR4-TANGO. N = 3 independent experiments. (b) β -arrestin 2 recruitment assay (PRESTO-Tango). Open symbols: cells transfected with FLAG-CXCR4/pcDNA3. Grey symbols: cells transfected with FLAG-CXCR4/ α_{1b} -AR. Cells were stimulated with phenylephrine (PE, circles) or CXCL12 (squares). N = 4 independent experiments. (c) β -arrestin 2 recruitment assay (PRESTO-Tango). Grey squares: cells transfected with FLAG-CXCR4-TANGO/ α_{1b} -AR. Grey circles: cells transfected with FLAG-CXCR4-TANGO/ α_{1b} -AR-TANGO. Open squares: cells transfected with FLAG-CXCR4-TANGO/pcDNA3. Open circles: cells transfected with α_{1b} -AR-TANGO/CXCR4. N = 3 independent experiments.

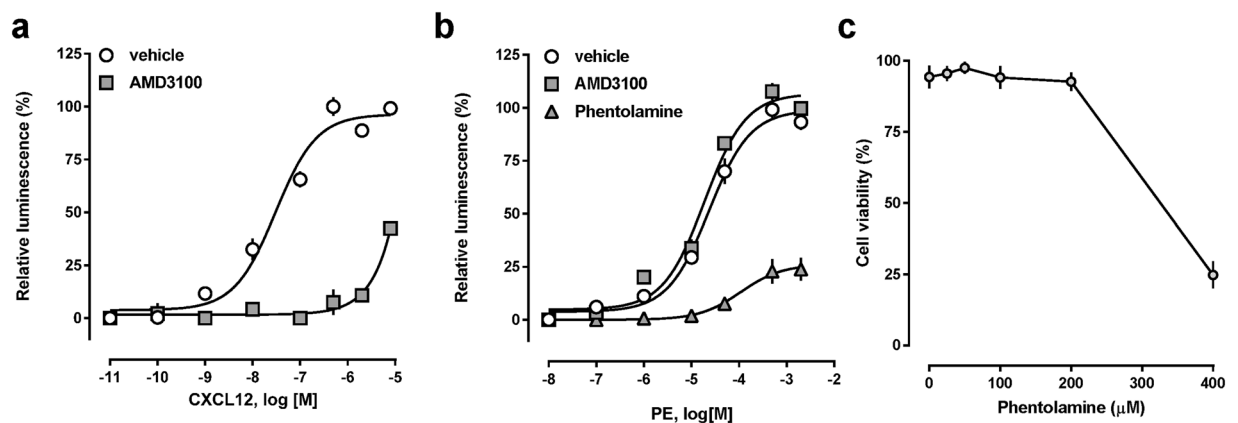


Figure 4. Effects of receptor antagonists on cross-recruitment of β -arrestin 2 to CXCR4 upon α_{1b} -AR activation. PE: phenylephrine. (a) β -arrestin 2 recruitment assay (PRESTO-Tango). Cells were transfected with FLAG-CXCR4-TANGO/pcDNA3 and stimulated with CXCL12 in the presence of vehicle (open circles) or AMD3100 (10 μ M). N = 3 independent experiments. (b) β -arrestin 2 recruitment assay (PRESTO-Tango). Cells were transfected with FLAG-CXCR4-TANGO/ α_{1b} -AR and stimulated with PE after pre-treatment (15 min, 37 $^{\circ}$ C) with vehicle (open circles), AMD3100 (10 μ M) or phentolamine (100 μ M). N = 3 independent experiments. (c) Cells were treated with various concentrations of phentolamine, as in b., and cell viability was determined by trypan blue exclusion. N = 3 independent experiments.

significantly increased the efficacy of PE to recruit β -arrestin 2 in cells co-expressing α_{1b} -AR-Tango and CXCR4 (top plateau: vehicle – 29.8 \pm 4.2%; TM2 – 60 \pm 3.8%, p = 0.0101) (Fig. 5e). These findings are consistent with the assumption that cross-recruitment of β -arrestin 2 to CXCR4 upon α_{1b} -AR activation depends on the formation of α_{1b} -AR:CXCR4 heteromers.

Recombinant CXCR4 internalizes upon agonist binding to α_{1b} -AR. Because β -arrestin recruitment to CXCR4 upon CXCL12 binding leads to internalization of the receptor, we then studied by immunofluorescence microscopy whether activation of α_{1b} -AR would also result in the internalization of CXCR4 in cells co-expressing

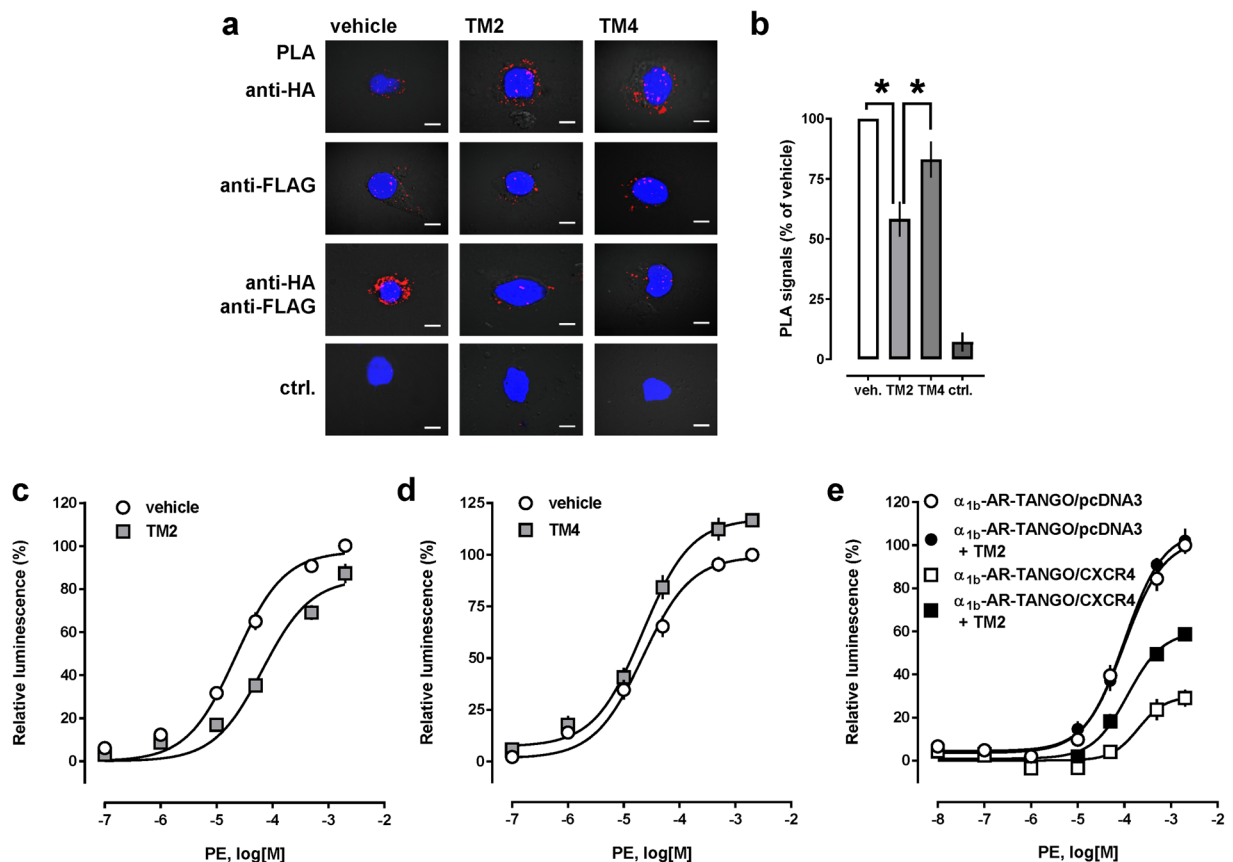


Figure 5. Effects of peptide analogues of transmembrane domains of CXCR4 on cross-recruitment of β -arrestin 2 to CXCR4 upon α_{1b} -AR activation. **(a)** Cells were co-transfected with HA- α_{1b} -AR and FLAG-CXCR4, treated with vehicle or peptide analogues of transmembrane domain (TM) 2 and TM4 (50 μ M, 15 min, 37 $^{\circ}$ C), and used for PLA. Typical PLA images for the detection of (from top to bottom) HA- α_{1b} -AR, FLAG-CXCR4 and interactions between both receptors are shown. Ctrl.: control, cells transfected with empty vector and stained for interactions between HA- α_{1b} -AR and FLAG-CXCR4. Scale bars: 10 μ m. **(b)** Quantification of PLA signals for FLAG-CXCR4-TANGO/HA- α_{1b} -AR interactions from $n = 3$ independent experiments, as in a. PLA signals/cell are expressed as % of vehicle treated cells. * $p < 0.05$ vs. cells incubated with TM2. **(c)** β -arrestin 2 recruitment assay (PRESTO-Tango). Cells were transfected with FLAG-CXCR4-TANGO/ α_{1b} -AR and stimulated with PE after pre-treatment (15 min, 37 $^{\circ}$ C) with vehicle (open circles) or the TM2 (50 μ M) peptide (grey squares). $N = 5$ independent experiments. **(d)** β -arrestin 2 recruitment assay (PRESTO-Tango). Cells were transfected with FLAG-CXCR4-TANGO/ α_{1b} -AR and stimulated with PE after pre-treatment (15 min, 37 $^{\circ}$ C) with vehicle (open circles) or the TM4 (50 μ M) peptide (grey squares). $N = 4$ independent experiments. **(e)** β -arrestin 2 recruitment assay (PRESTO-Tango). Cells were transfected as indicated and stimulated with PE after pre-treatment (15 min, 37 $^{\circ}$ C) with vehicle (open symbols) or the TM2 (50 μ M) peptide (black symbols). $N = 3$ independent experiments.

both recombinant receptors. After transfection with HA-CXCR4 plus pcDNA3 or α_{1b} -AR, HEK293T cells were labeled with FITC-conjugated anti-HA at 4 $^{\circ}$ C, followed by stimulation with vehicle, CXCL12 or PE at room temperature. In cells co-expressing HA-CXCR4 and pcDNA3 (Fig. 6a), the fluorescence signal for FITC-labeled anti-HA was localized to the cell membrane after vehicle and PE treatment (left and right). After treatment with CXCL12, punctate areas of fluorescence were detectable, indicating internalization of HA-CXCR4 (center). In cells co-expressing HA-CXCR4 and α_{1b} -AR (Fig. 6b), CXCL12 and PE treatment resulted in punctate areas of fluorescence, suggesting that HA-CXCR4 internalizes upon activation of α_{1b} -AR. Measurements of cell surface HA-CXCR4 expression levels by flow cytometry confirmed these observations and showed that PE did not affect HA-CXCR4 expression levels in cells co-expressing HA-CXCR4/pcDNA3 (Fig. 6c), but reduced HA-CXCR4 expression levels in cells co-expressing HA-CXCR4/ α_{1b} -AR (Fig. 6d).

CXCR4 in human vascular smooth muscle cells internalizes upon agonist binding to α_1 -AR. To assess whether PE stimulation also induces internalization of endogenous CXCR4, we then incubated hVSMC with rabbit anti-CXCR4 ACR-014 at 4 $^{\circ}$ C, followed by incubation with vehicle, CXCL12 or PE at 37 $^{\circ}$ C. Cells were then fixed, permeabilized and incubated with Alexa488-conjugated goat anti-rabbit IgG. Fluorescence microscopy showed a diffuse pattern of fluorescence in vehicle treated cells (Fig. 7a, left column, top). In cells treated with CXCL12 and PE (Fig. 7a, left column, center and bottom), bright fluorescent punctate areas were visible.

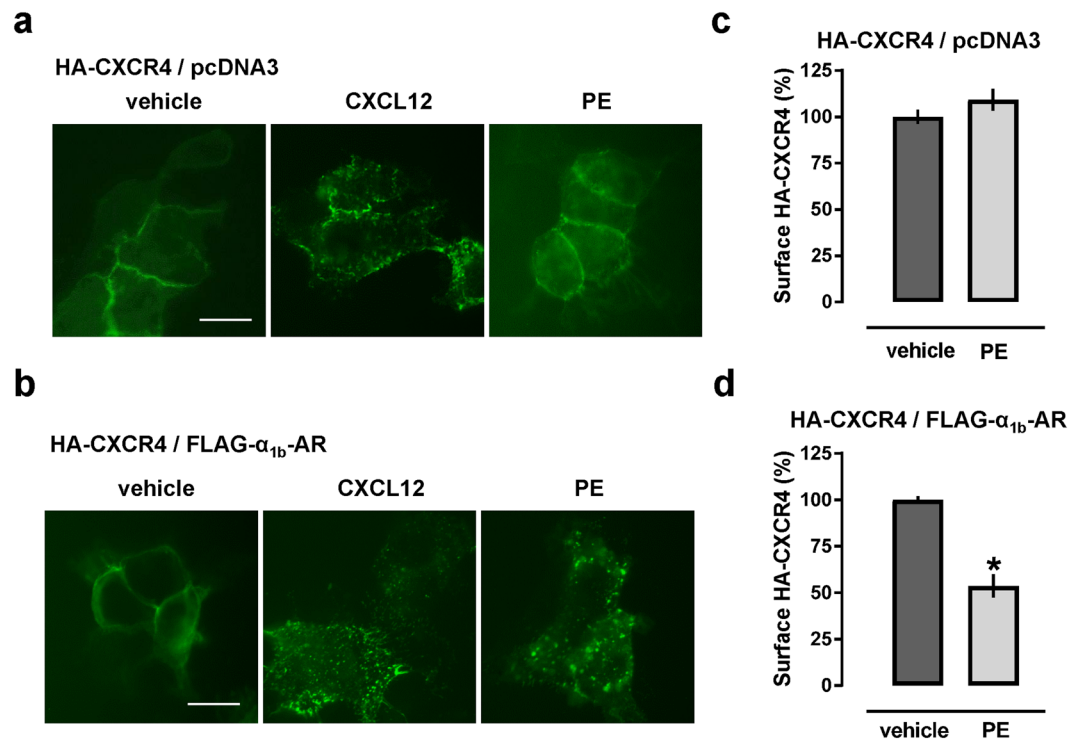


Figure 6. α_{1b} -AR activation within the CXCR4: α_{1b} -AR heteromer leads to internalization of CXCR4 in HEK293T cells. (a,b) After labeling HA-CXCR4 with FITC-conjugated anti-HA at 4 °C, HEK293T cells were treated with CXCL12 (200 nM) or phenylephrine (PE, 200 μ M) for 1 hour at room temperature. Images are representative of $n = 3$ independent experiments. Scale bar: 20 μ m. HEK293T cells were transfected with HA-CXCR4/pcDNA3 (a) or with HA-CXCR4/FLAG- α_{1b} -AR (b). (c,d) Quantification of HA-CXCR4 cell surface expression by flow cytometry with FITC-anti-HA in cells after stimulation with PE, as in a/b. Cells were transfected with HA-CXCR4/pcDNA3 (c) or HA-CXCR4/ α_{1b} -AR (d). Surface HA-CXCR4 expression is expressed as % fluorescence intensity of cells treated with vehicle. * $p < 0.05$ vs. vehicle. $N = 4$ independent experiments.

These observations are consistent with CXCR4 internalization and with the staining patterns that have previously been observed in similar fluorescence microscopy internalization studies of other GPCRs¹⁹. When these experiments were performed with FITC-labeled anti-CXCR4 12G5, an antibody known to inhibit CXCL12 binding to CXCR4²⁰, fluorescent punctate formation did not occur after CXCL12 treatment, but persisted after PE treatment (Fig. 7a, right column). These findings are in line with our observation that blockade of CXCR4 with AMD3100 did not prevent β -arrestin 2 cross-recruitment upon α_{1b} -AR activation (Fig. 4b). To confirm that PE treatment leads to internalization of CXCR4 in hVSMC, we then performed PLA to analyze expression levels of CXCR4, α_{1b} -AR and CXCR4: α_{1b} -AR heteromers after vehicle and PE treatment (Fig. 7b). The quantification of the PLA signals per cell from three independent experiments is shown in Fig. 7c. As compared with vehicle treated cells, PLA signals corresponding to CXCR4, α_{1b} -AR and heteromeric CXCR4: α_{1b} -AR complexes were significantly reduced after PE treatment. Together, our observations suggest that activation of α_{1b} -AR within the α_{1b} -AR:CXCR4 heteromer recruits β -arrestin to both receptor partners, leading to co-internalization of α_{1b} -AR and CXCR4. Furthermore, our findings that AMD3100 and anti-CXCR4 12G5 did not prevent β -arrestin 2 recruitment and internalization of CXCR4 upon PE stimulation indicate that this receptor cross-talk can occur when CXCR4 is in its ligand-free and in an antagonist-bound configuration. This assumption is supported by the recent observation that chemically-induced fusion of CXCR4 to β -arrestin 1/2 leads to internalization of the receptor, independent of agonist binding to and G protein coupling through CXCR4²¹.

Ligand binding to α_1 -AR inhibits CXCR4-mediated chemotaxis of human vascular smooth muscle cells.

To assess consequences of ligand binding to α_1 -AR on CXCR4-mediated effects on cell function, we then studied chemotactic responses of hVSMC in trans-well migration assays. We reported previously that the dose-response profile of CXCL12 shows maximal chemotactic activity at concentrations between 10–100 nM in hVSMC under our experimental conditions²². As expected^{23,24}, PE also dose-dependently induced chemotaxis in hVSMC under these conditions (Fig. 7d). Maximal chemotactic activity of PE was comparable with the chemotactic activity of CXCL12. When hVSMC were loaded onto the membrane in the presence of increasing concentrations of PE, migration towards 10 nM CXCL12 was significantly reduced. At a concentration of 10 nM PE, chemotaxis towards 10 nM CXCL12 was reduced by more than 50% and further increases in PE concentrations dose-dependently reduced the chemotactic index (CI) to 20% of the CI in the absence of PE (dark grey bars). When hVSMC migrated towards 10 nM CXCL12 plus increasing concentrations of PE, PE inhibited chemotaxis

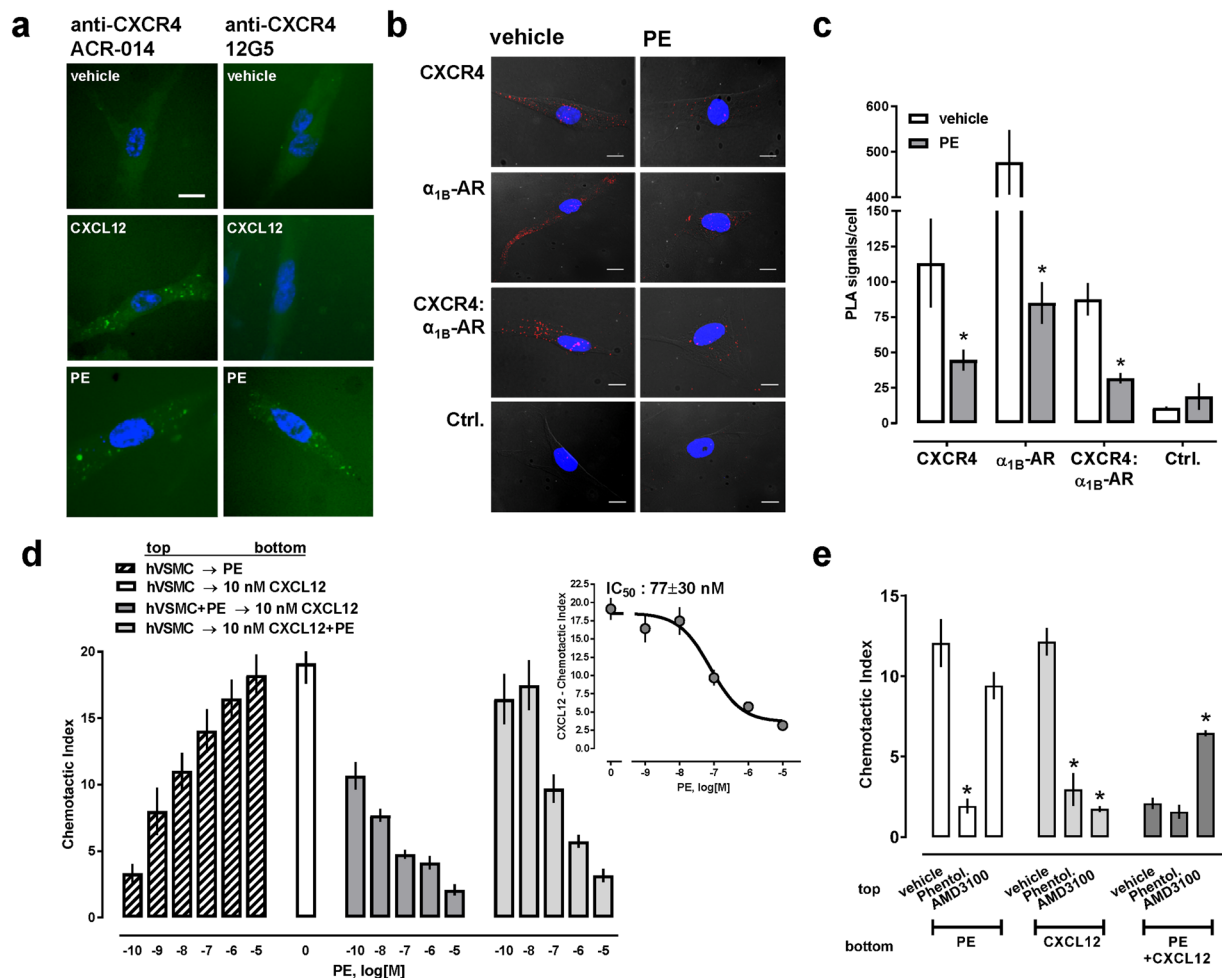


Figure 7. α_1 -AR regulate internalization of CXCR4 in human vascular smooth muscle cells and CXCR4-mediated chemotaxis. **(a)** hVSMC were labeled for 1 hour at 4 °C with rabbit anti-CXCR4 (ACR-014, left) or FITC-conjugated-anti-CXCR4 (12G5, right), and then treated with vehicle, 100 nM CXCL12 or 10 μ M PE for 20 min at 37 °C. Cells stained with anti-CXCR4 (ACR-014) were permeabilized with TX-100 and stained with Alexa 488-conjugated anti-rabbit. Fluorescence microscopy images are representative of $n = 3$ independent experiments. Scale bar: 20 μ m. **(b)** Representative PLA images for the detection of individual receptors and receptor-receptor interactions in hVSMC. Cells were treated with vehicle or PE (1 μ M) for 15 min at 37 °C. Ctrl.: Omission of one primary antibody. Images show merged PLA/4',6-diamidino-2-phenylindole dihydrochloride signals. Scale bars = 10 μ m. **(c)** Quantification of PLA signals, as in b. $N = 3$ with $n = 10$ images per condition and experiment. * $p < 0.05$ vs. ctrl. **(d)** Migration of hVSMC towards PE (hatched bars), CXCL12 (10 nM, open bar) and combinations of both (grey bars). Dark grey bars: migration of hVSMC in the presence of various concentrations of PE towards 10 nM CXCL12. Light grey bars: migration of hVSMC towards 10 nM CXCL12 plus various concentrations of PE (insert shows the dose-response curve). $N = 4$ independent experiments. **(e)** hVSMC were pre-treated with 10 μ M phentolamine, 10 μ M AMD3100, or vehicle for 15 min at room temperature, followed by migration towards 1 μ M PE, 10 nM CXCL12, or both. $N = 4$ independent experiments. * $p < 0.05$ vs. vehicle.

with an IC₅₀ of 77 \pm 30 nM (Fig. 7d, dark grey bars and inset). These findings are in agreement with previous observations on the pharmacological behaviors of the CXCR4: δ -opioid receptor and CXCR4:cannabinoid receptor 2 heteromers, in which agonist co-stimulation of both receptor partners abolished chemotaxis towards CXCL12^{13,14}.

As pharmacological cross-inhibition has previously been described for other GPCR heteromers, we then tested the effects of AMD3100 and phentolamine on the chemotactic responses of hVSMC to CXCL12, PE and a combination of both agonists. As in Fig. 7d, hVSMC migrated towards PE and CXCL12 and this response was inhibited when cells migrated towards both agonists (Fig. 7e). Phentolamine inhibited PE- and CXCL12-induced chemotaxis, but did not alter the chemotactic response to both agonists. In contrast, AMD3100 inhibited CXCL12-induced chemotaxis, but did not significantly affect PE-induced chemotaxis. AMD3100, however, restored a chemotactic response of hVSMC to the combination of PE and CXCL12. In combination with the effects of PE on β -arrestin 2 cross-recruitment to and co-internalization of CXCR4, these findings indicate

asymmetrical cross-activation and cross-inhibition of CXCR4 within the heteromeric receptor complex by α_1 -AR ligands. Such a pharmacological behavior of the CXCR4: α_1 -AR heteromeric complex is similar to the signaling behavior of other GPCR heteromers, for which both ligand-induced symmetrical and asymmetrical cross-activation and cross-inhibition of various signaling read-outs have previously been described^{25–28}. For example, symmetrical ligand induced cross-inhibition and cross-sensitization was observed for the angiotensin II receptor type 1:prostaglandin F₂ α receptor heteromer when aortic ring contraction was used as a functional read-out, whereas the effects of agonist stimulation on [³H]thymidine incorporation in vascular smooth muscle cells showed asymmetrical cross-inhibition, i.e. a prostaglandin F₂ α receptor antagonist inhibited angiotensin II-induced effects but an angiotensin II receptor type 1 antagonist did not affect prostaglandin F₂ α induced-effects. Similarly, agonist-induced cross-phosphorylation and cross-internalization was observed at the NK1 receptor: μ -opioid receptor heteromer²⁵.

It has been proposed previously that simultaneous agonist binding to both receptor partners can inhibit signaling of heteromeric receptor complexes, such as the CXCR4:cannabinoid receptor 2, CXCR4: δ -opioid receptor or μ -opioid receptor:CCR5 heteromers^{13,14,29}. As the results from the present study point towards β -arrestin 2 cross-recruitment to AMD3100-bound CXCR4 upon α_1 -AR activation, a possible explanation for the observation that AMD3100 restored chemotaxis of hVSMC towards both agonists is that coupling of the heteromeric receptor complex to both G α_i and G α_q upon ligand binding is required to prevent PE-induced chemotaxis. The finding that phentolamine did not restore chemotaxis of hVSMC towards both agonists is not contradictory because phentolamine cross-inhibited chemotactic responses of hVSMC towards CXCL12 alone.

In conclusion, our findings provide new mechanistic insights into molecular signaling events at the CXCR4: α_{1b} -AR hetero-oligomeric complex and evidence that α_1 -ARs regulate CXCR4-mediated functions in hVSMC. Our findings of asymmetrical agonist- and antagonist-induced cross-regulation of CXCR4 by α_1 -AR within the heteromeric receptor complex have several implications. While these data provide a mechanistic basis for interactions between the neuroendocrine and immune system, our findings also point towards α_1 -AR as new pharmacological target to modulate CXCR4 expression levels and CXCR4-mediated effects on cell migration in various disease processes, such as cancer metastasis or autoimmune diseases. These data further support the notion that the development of drugs which selectively target heteromeric receptor complexes could have novel and unique pharmacological properties and also imply that drugs with high selectivity for a specific GPCR can have unforeseen pharmacological effects through its actions on heteromerization receptor partners. Thus, the detailed elucidation of the molecular properties of heteromeric receptor complexes will provide new opportunities for drug development and may also help to better anticipate unwanted side-effect profiles of drugs targeting GPCRs.

Methods

Proteins, peptides and reagents. Phenylephrine, phentolamine and AMD3100 were purchased from Sigma Aldrich. CXCL12 was from Protein Foundry. The peptide analogs of transmembrane helix 2 (TM2) and TM4 of CXCR4 were as previously described¹⁷.

Cells. Human vascular smooth muscle cells (hVSMC; primary aortic smooth muscle cells, ATCC-PCS-100-012) and HEK 293 T cells (ATCC-CRL-11268) were purchased from American Type Culture Collection. hVSMC were cultured in vascular basal media (ATCC PCS-100-030) supplemented with the vascular smooth muscle growth kit (ATCC PCS-100-042), 100 U/mL penicillin, 100 μ g/mL streptomycin. hVSMCs were used between passages 2–5. HEK 293 T cells were cultured in high-glucose Dulbecco's Modified's Eagle Medium containing 10 mg/mL sodium pyruvate, 2 mM L-glutamine, 10% FBS, 100 U/mL penicillin, and 100 μ g/mL streptomycin. The HTLA cell line, a HEK293 cell line stably expressing a tTA-dependent luciferase reporter and a β -arrestin2-TEV fusion gene¹⁸, was generously provided by the laboratory of Dr. Bryan Roth and maintained in high glucose Dulbecco's Modified's Eagle Medium supplemented with 10% FBS, 100 U/mL penicillin, 100 μ g/mL streptomycin, 100 μ g/mL hygromycin B, and 2 μ g/mL puromycin. All cells were cultured in a humidified environment at 37°C, 5% CO₂.

Flow cytometry. Flow cytometry after labeling cells with Phycoerythrin-conjugated anti-FLAG antibody (Biolegend, 637310), Alexa 647-conjugated anti-FLAG antibody (R&D, IC8529R), Alexa 488-conjugated anti-Myc antibody (R&D, IC3696G) or FITC-conjugated anti-HA antibody (Sigma-Aldrich, H7411) was used to quantify recombinant receptor expression levels in HEK293T cells, as described^{15,30,31}. At least 10,000 cells/sample were recorded and analyzed with the FlowJo software (Tree Star).

Proximity Ligation Assays (PLA). PLA were performed as described in detail previously^{15,16}. To visualize individual receptors, slides were incubated with mouse anti-FLAG M2 (Sigma-Aldrich, F1804), rabbit anti-HA (Abcam, Ab9110), rabbit anti- α_{1B} -AR (Abcam Ab169523) or goat anti-CXCR4 (Abcam Ab1670) at 37°C for 105 min in a humidifying chamber at 37°C. Anti- α_{1B} -AR and anti-CXCR4 have been validated for sufficient selectivity previously^{16,31}. Slides were then washed and incubated (1 h, 37°C) with secondary species specific (rabbit/mouse/goat) antibodies conjugated with plus and minus Duolink II PLA probes (1:5), as appropriate. To visualize receptor-receptor interactions, slides were incubated with a combination of rabbit anti- α_{1B} -AR (Abcam Ab169523) and goat anti-CXCR4 (Abcam Ab1670) or a combination of mouse anti-FLAG M2 and rabbit anti-HA. All antibodies, except anti-HA (dilution 1:1000), were used in dilutions of 1:500. Slides were then washed and incubated with secondary species specific antibodies conjugated with plus and minus Duolink II PLA probes (1:5) corresponding to the two primary antibodies. PLA signals were quantified using the Duolink Image Tool software (Sigma Aldrich). Comparisons and statistical analyses were performed only when PLA assays were performed on the same day in parallel experiments and fluorescence microscopy was performed with the identical settings. For each experiment and condition, 10 randomly selected non-overlapping vision fields were analyzed.

Plasmids and transfections. FLAG-tagged Tango plasmids (CXCR4-TANGO, #66262; α_{1b} -AR-TANGO, #66214; α_{1d} -TANGO, #66215) were from Addgene deposited by the laboratory of Dr. Bryan Roth. Myc-tagged TANGO plasmids were generated by replacing the original FLAG-tag plasmids with Myc tag after PCR amplification with primers carrying the Myc tag sequence. HA- or FLAG-tagged CXCR4, α_{1b} -AR or α_{1d} -AR were generated by PCR amplification using corresponding TANGO plasmids as cDNAs with primers carrying Xho I and Xba I sites and inserted in pcDNA3 with an N-terminal FLAG or HA tag. All plasmids were verified by sequencing. HEK293T cells were transiently transfected with a single DNA or two DNAs that encode HA- or FLAG-tagged CXCR4, α_{1b} -AR or α_{1d} -AR or TANGO plasmids at the amounts indicated, using Lipofectamine 3000 (Thermo Scientific) as per manufacturer's protocol. For single GPCR-encoding DNA transfection, empty vector pcDNA3 was added to maintain the total DNA amount per transfection constant.

PRESTO-Tango β -arrestin recruitment assay. The PRESTO-Tango (parallel receptorome expression and screening via transcriptional output, with transcriptional activation following arrestin translocation) assay was performed as recently described¹⁸. HTLA cells (2.5×10^5 /well) were seeded in a 6-well plate and transfected with 750 ng of each of the Tango plasmids using Lipofectamine 3000 (Thermo Scientific). The following day, transfected HTLA cells (75,000 cells/well) were plated onto Poly-L-Lysine pre-coated 96-well microplates and allowed to attach to the plate surface for at least 4 hours prior to treatment. Cells were treated with receptor agonists for 2 h and then replaced with fresh full medium and incubated overnight at 37 °C, 5% CO₂ in a humidified environment. To test the effects of TM peptides (50 μ M), AMD3100 (10 μ M) or phentolamine (100 μ M), cells were pre-incubated with these reagents for 15 min at 37 °C before adding agonists. The following morning, medium was removed from cell culture plates and replaced with a 100 μ L 1:5 mixture of Bright-Glo (Promega) and 1 \times HBSS, 20 mM HEPES solution. Plates were then incubated at room temperature for 20 min before measuring luminescence on a Biotek Synergy II plate reader. Relative luminescence (RLU) is expressed as % of luminescence upon stimulation with the highest concentration of the corresponding receptor agonist when the Tango receptor was co-expressed with pcDNA3 (=100%). When HTLA cells were not transfected with a Tango plasmid, no change in luminescence was detectable upon agonist treatment (Supplementary Fig. S3).

Immunofluorescence receptor internalization assays. Receptor internalization assays were performed with HEK293T cells and hVSMC. HEK293T cells were transfected with HA-CXCR4 plus pcDNA3 or FLAG- α_{1b} -AR at 375 ng each DNA/well of a 12-well plate. After 24 hours, cells were re-plated in poly D-lysine coated 8-well chamber slides. After overnight incubation, cells were chilled on ice and labeled with FITC-conjugated anti-HA (Sigma-Aldrich, H7411, 2 μ g/ml in Opti-MEM) for 1 h at 4 °C. Subsequently, labeled cells were washed with Opti-MEM twice and then incubated with CXCL12 (200 nM) or PE (200 μ M) for 1 h at room temperature. Thereafter, cells were washed with PBS and fixed with 4% paraformaldehyde. hVSMC were plated in 8-well chamber slides. The next day, slides were cooled on ice, washed once with Opti-MEM and then incubated with FITC-conjugated anti-CXCR4 antibody (R&D, FAB170F, 1:150 dilution in Opti-MEM) or rabbit anti-CXCR4 antibody (Alomone, ACR-014, 1:150 in Opti-MEM) at 4 °C for 1 h. Subsequently, slides were washed twice and then treated with CXCL12 (100 nM) or PE (10 μ M) in Opti-MEM at 37 °C for 20 min. Cells were fixed with 4% paraformaldehyde/PBS at room temperature for 10 min. After three washes with PBS, cells incubated with non-conjugated anti-CXCR4 were permeabilized with 0.2% Triton X-100/PBS at room temperature for 10 min and then blocked with 1% BSA/PBS for 30 min, followed by incubation with Alexa 488-conjugated goat anti-rabbit antibody (1:250) at room temperature for 1 h. HEK293T cells and hVSMC Cells were mounted with mounting medium for fluorescence microscopy. Images were obtained under a fluorescence microscope (Carl Zeiss Axiovert 200 M) with a 40x objective lens equipped with Axio CamMRc5. For each well, 10 vision fields were imaged.

Chemotaxis assays. Cell migration was assessed using the ChemoTx 96-well cell migration system, as described^{17,22,32}. The chemotactic index (CI) was calculated as the ratio of cells that transmigrated through the filter in the presence versus the absence (=PBS/control) of the test solutions.

Cell viability assays. Cell viability was assessed using the Trypan blue exclusion method. HTLA cells were incubated with various concentrations of phentolamine under the same conditions used in Presto-Tango assays. After staining cells with Trypan blue, at least 100 cells per condition and experiment were examined in a hemocytometer and the percentage of viable cells quantified.

Data analyses. Data are expressed as mean \pm standard error of the mean (SEM) from n independent experiments that were performed on different days. Data were analyzed using the GraphPad-Prism 7 software. Unpaired Student's t test or one-way analyses of variance (ANOVA) with Dunnett's multiple comparison post-hoc test for multiple comparisons were used, as appropriate. Dose response curves were generated using non-linear regression analyses. A two-tailed $p < 0.05$ was considered significant.

Data availability. The datasets generated during the current study are available from the corresponding author on reasonable request.

References

- Bachelier, F. *et al.* International Union of Pharmacology. LXXXIX. Update on the extended family of chemokine receptors and introducing a new nomenclature for atypical chemokine receptors. *Pharmacol. Rev.* **66**, 1–79 (2014).
- Teicher, B. A. & Fricker, S. P. CXCL12 (SDF-1)/CXCR4 pathway in cancer. *Clin. Cancer Res.* **16**, 2927–2931 (2010).
- Nagasawa, T., Tachibana, K. & Kishimoto, T. A novel CXC chemokine PBSF/SDF-1 and its receptor CXCR4: their functions in development, hematopoiesis and HIV infection. *Semin. Immunol.* **10**, 179–185 (1998).
- Pozzobon, T., Goldoni, G., Viola, A. & Molon, B. CXCR4 signaling in health and disease. *Immunol. Lett.* **177**, 6–15 (2016).

5. Barbieri, F., Bajetto, A., Thellung, S., Wurth, R. & Florio, T. Drug design strategies focusing on the CXCR4/CXCR7/CXCL12 pathway in leukemia and lymphoma. *Expert Opin. Drug Discov.* **11**, 1093–1109 (2016).
6. Busillo, J. M. & Benovic, J. L. Regulation of CXCR4 signaling. *Biochim. Biophys. Acta* **1768**, 952–963 (2007).
7. Watts, A. O. *et al.* Identification and profiling of CXCR3–CXCR4 chemokine receptor heteromer complexes. *Br. J. Pharmacol.* **168**, 1662–1674 (2013).
8. Sohy, D. *et al.* Hetero-oligomerization of CCR2, CCR5, and CXCR4 and the protean effects of “selective” antagonists. *J. Biol. Chem.* **284**, 31270–31279 (2009).
9. LaRocca, T. J. *et al.* beta2-Adrenergic receptor signaling in the cardiac myocyte is modulated by interactions with CXCR4. *J. Cardiovasc. Pharmacol.* **56**, 548–559 (2010).
10. de Poorter, C. *et al.* Consequences of ChemR23 heteromerization with the chemokine receptors CXCR4 and CCR7. *PLoS One* **8**, e58075 (2013).
11. Sohy, D., Parmentier, M. & Springael, J. Y. Allosteric transinhibition by specific antagonists in CCR2/CXCR4 heterodimers. *J. Biol. Chem.* **282**, 30062–30069 (2007).
12. Decailott *et al.* CXCR7/CXCR4 heterodimer constitutively recruits beta-arrestin to enhance cell migration. *J. Biol. Chem.* **286**, 32188–32197 (2011).
13. Pello, O. M. *et al.* Ligand stabilization of CXCR4/delta-opioid receptor heterodimers reveals a mechanism for immune response regulation. *Eur. J. Immunol.* **38**, 537–549 (2008).
14. Coke, C. J. *et al.* Simultaneous Activation of Induced Heterodimerization between CXCR4 Chemokine Receptor and Cannabinoid Receptor 2 (CB2) Reveals a Mechanism for Regulation of Tumor Progression. *J. Biol. Chem.* **291**, 9991–10005 (2016).
15. Tripathi, A. *et al.* Heteromerization of chemokine (C-X-C motif) receptor 4 with alpha1A/B-adrenergic receptors controls alpha1-adrenergic receptor function. *Proc. Natl. Acad. Sci. USA* **112**, E1659–1668 (2015).
16. Albee, L. J. *et al.* alpha1-Adrenoceptors function within hetero-oligomeric complexes with chemokine receptors ACKR3 and CXCR4 in vascular smooth muscle cells. *J. Am. Heart Assoc.* **6**, e006575 (2017).
17. Evans, A. E. *et al.* New Insights into Mechanisms and Functions of Chemokine (C-X-C Motif) Receptor 4 Heteromerization in Vascular Smooth Muscle. *Int. J. Mol. Sci.* **17**, E971 (2016).
18. Kroeze, W. K. *et al.* PRESTO-Tango as an open-source resource for interrogation of the druggable human GPCRome. *Nat. Struct. Mol. Biol.* **22**, 362–369 (2015).
19. Lutz, W., Sanders, M., Salisbury, J. & Kumar, R. Internalization of vasopressin analogs in kidney and smooth muscle cells: evidence for receptor-mediated endocytosis in cells with V2 or V1 receptors. *Proc. Natl. Acad. Sci. USA* **87**, 6507–6511 (1990).
20. Hesselgesser, J. *et al.* Identification and characterization of the CXCR4 chemokine receptor in human T cell lines: ligand binding, biological activity, and HIV-1 infectivity. *J. Immunol.* **160**, 877–883 (1998).
21. Liebick, M., Henze, S., Vogt, V. & Oppermann, M. Functional consequences of chemically-induced beta-arrestin binding to chemokine receptors CXCR4 and CCR5 in the absence of ligand stimulation. *Cell Signal.* **38**, 201–211 (2017).
22. Eby, J. M. *et al.* Functional and structural consequences of chemokine (C-X-C motif) receptor 4 activation with cognate and non-cognate agonists. *Mol. Cell Biochem.* Apr 28. <https://doi.org/10.1007/s11010-017-3044-7>. [Epub ahead of print] (2017).
23. Nishio, E. & Watanabe, Y. The involvement of reactive oxygen species and arachidonic acid in alpha 1-adrenoceptor-induced smooth muscle cell proliferation and migration. *Br. J. Pharmacol.* **121**, 665–670 (1997).
24. Zhang, H., Facemire, C. S., Banes, A. J. & Faber, J. E. Different alpha-adrenoceptors mediate migration of vascular smooth muscle cells and adventitial fibroblasts *in vitro*. *Am. J. Physiol. Heart Circ. Physiol.* **282**, H2364–2370 (2002).
25. Pfeiffer, M. *et al.* Heterodimerization of substance P and mu-opioid receptors regulates receptor trafficking and resensitization. *J. Biol. Chem.* **278**, 51630–51637 (2003).
26. Ferre, S. *et al.* G protein-coupled receptor oligomerization revisited: functional and pharmacological perspectives. *Pharmacol. Rev.* **66**, 413–434 (2014).
27. Martinez-Pinilla, E. *et al.* Dopamine D2 and angiotensin II type 1 receptors form functional heteromers in rat striatum. *Biochem. Pharmacol.* **96**, 131–142 (2015).
28. Goupil, E. *et al.* Angiotensin II type I and prostaglandin F2alpha receptors cooperatively modulate signaling in vascular smooth muscle cells. *J. Biol. Chem.* **290**, 3137–3148 (2015).
29. Chen, C. *et al.* Heterodimerization and cross-desensitization between the mu-opioid receptor and the chemokine CCR5 receptor. *Eur. J. Pharmacol.* **483**, 175–186 (2004).
30. Saini, V., Marchese, A. & Majetschak, M. CXC chemokine receptor 4 is a cell surface receptor for extracellular ubiquitin. *J. Biol. Chem.* **285**, 15566–15576 (2010).
31. Tripathi, A., Gaponenko, V. & Majetschak, M. Commercially available antibodies directed against alpha-adrenergic receptor subtypes and other G protein-coupled receptors with acceptable selectivity in flow cytometry experiments. *Naunyn Schmiedeberg's Arch. Pharmacol.* **389**, 243–248 (2016).
32. Saini, V. *et al.* The CXC chemokine receptor 4 ligands ubiquitin and stromal cell-derived factor-1alpha function through distinct receptor interactions. *J. Biol. Chem.* **286**, 33466–33477 (2011).

Acknowledgements

This work was supported by the National Institute of General Medical Sciences (Award R01GM107495) and by the National Cancer Institute (Award R01CA188427). The content is solely the responsibility of the authors and does not necessarily represent the official views of the National Institutes of Health.

Author Contributions

X.G. and M.M. conceived and designed experiments. X.G. and L.J.A. performed experiments. X.G., L.J.A. and M.M. analyzed data. B.F.V. and V.G. provided reagents. M.M. wrote the manuscript. All authors reviewed and commented on the manuscript and approved the final version.

Additional Information

Supplementary information accompanies this paper at <https://doi.org/10.1038/s41598-018-21096-4>.

Competing Interests: Based on this study, Loyola University Chicago has filed a provisional patent application. X.G., L.J.A. and M.M. are inventors.

Publisher's note: Springer Nature remains neutral with regard to jurisdictional claims in published maps and institutional affiliations.



Open Access This article is licensed under a Creative Commons Attribution 4.0 International License, which permits use, sharing, adaptation, distribution and reproduction in any medium or format, as long as you give appropriate credit to the original author(s) and the source, provide a link to the Creative Commons license, and indicate if changes were made. The images or other third party material in this article are included in the article's Creative Commons license, unless indicated otherwise in a credit line to the material. If material is not included in the article's Creative Commons license and your intended use is not permitted by statutory regulation or exceeds the permitted use, you will need to obtain permission directly from the copyright holder. To view a copy of this license, visit <http://creativecommons.org/licenses/by/4.0/>.

© The Author(s) 2018